processes

Article

A Novel Hybrid Approach for Modeling and Optimisation of Phosphoric Acid Production through the Integration of AspenTech, SciLab Unit Operation, Artificial Neural Networks and Genetic Algorithm

Marko Pavlović [1], Jelena Lubura [1], Lato Pezo [2], Milada Pezo [3], Oskar Bera [1] and Predrag Kojić [1,*]

[1] Faculty of Technology Novi Sad, University of Novi Sad, Bulevar cara Lazara 1, 21000 Novi Sad, Serbia; jelenalubura@uns.ac.rs (J.L.); obera@uns.ac.rs (O.B.)
[2] Institute of General and Physical Chemistry, University of Belgrade, Studentski Trg 12-16, 11000 Belgrade, Serbia; latopezo@yahoo.co.uk
[3] Laboratory for Thermal Engineering and Energy, Institute of Nuclear Sciences "Vinča", University of Belgrade, P.O. Box 522, 11001 Belgrade, Serbia; milada@vinca.rs
* Correspondence: kojicpredrag@uns.ac.rs

Abstract: The purpose of the study was to identify and predict the optimized parameters for phosphoric acid production. This involved modeling the crystal reactor, UCEGO filter (as a detailed model of the filter is not available in Aspen Plus or other simulation software), and acid separator using Sci-Lab to develop Cape-Open models. The simulation was conducted using Aspen Plus and involved analyzing 10 different phosphates with varying qualities and fractions of P_2O_5 and other minerals. After a successful simulation, a sensitivity analysis was conducted by varying parameters such as capacity, filter speed, vacuum, particle size, water temperature for washing the filtration cake, flow of recycled acid and strong acid from the separator below the filter, flow of slurry to reactor 1, temperature in reactors, and flow of H_2SO_4, resulting in nearly one million combinations. To create an algorithm for predicting process parameters and the maximal extent of recovering H_3PO_4 from slurry, ANN models were developed with a determination coefficient of 99%. Multi-objective optimization was then performed using a genetic algorithm to find the most suitable parameters that would lead to a higher reaction degree (96–97%) and quantity of separated H_3PO_4 and lower losses of gypsum. The results indicated that it is possible to predict the influence of process parameters on the quality of produced acid and minimize losses during production. The developed model was confirmed to be viable when compared to results found in the literature.

Keywords: UCEGO filter; Aspen; artificial neural network; multi-objective optimization; genetic algorithm; phosphoric acid

Citation: Pavlović, M.; Lubura, J.; Pezo, L.; Pezo, M.; Bera, O.; Kojić, P. A Novel Hybrid Approach for Modeling and Optimisation of Phosphoric Acid Production through the Integration of AspenTech, SciLab Unit Operation, Artificial Neural Networks and Genetic Algorithm. *Processes* **2023**, *11*, 1753. https://doi.org/10.3390/pr11061753

Received: 4 May 2023
Revised: 29 May 2023
Accepted: 6 June 2023
Published: 8 June 2023

1. Introduction

The current global consumption of H_3PO_4 is on the rise, while the amount of basic raw material required for its production decreases each year. The world's reserves of phosphate rocks are limited, with a total of 65,000 million tons [1]. The increased demand for phosphoric acid in the food, mineral waste, and pharmaceutical industries is driving market growth. It is estimated that the global phosphoric acid market will reach USD 47,718.13 million by 2028 [2]. Based on these trends, the depletion of phosphate rock reserves will continue. Therefore, it is necessary to take action and implement cost-saving measures to prolong the increase in consumption for as long as possible.

Although there are alternative ways to produce phosphoric acid [1], they are cost prohibitive, especially for developing countries. Consequently, the most efficient approach would be to increase the utilization of P_2O_5 from phosphate rock and minimize losses of acid in gypsum to slow down the declining trend of phosphate.

The morphological composition and quality of phosphate ore vary depending on its geographical origin. Even neighboring mines can have different compositions, which presents a challenge in maximizing the utilization of its main component, P_2O_5. Various production methods for phosphoric acid (such as Hemihydrate, Dihydrate, dry process, etc.) can be found in the literature [3–13]. However, the most commonly used process for the production of phosphoric acid is the Dihydrate process [8]. Different compositions of phosphate ore can lead to varying results in UCEGO filtration and the reaction in the reactor. The filter is sensitive to factors such as crystal size and shape, viscosity, and density, which can affect the filtration and reaction processes. Additionally, the presence of organic components can result in the formation of a large amount of foam, which can clog the filter mesh and hinder filtration, resulting in a greater loss of phosphoric acid in the gypsum cake. The separation processes of H_3PO_4 from gypsum using UCEGO filters have received little attention in the literature. While books [14,15] provide detailed descriptions of the filter used in phosphoric acid production, research papers typically focus on the reaction, without emphasizing the importance of the filtration [4,6,9–12]. It should be mentioned that population modeling and optimization of phosphoric acid production are presented in [13], where multi-objective optimization (MO) was conducted with high precision (relative difference 0.01–4.5%).

The results of the investigations discussed in this study enable the attainment of a high yield of H_3PO_4 in the reactor, taking into account various parameters and conditions in the filtration section (UCEGO filter and separator) as empirical assumptions and predictions. It is important to note that the processes are simulated statically, while the filter and reactor conditions, as well as the composition of each material flow, are dynamic. This study takes into consideration the fact that phosphate ore is present in many varieties of composition and that small variations in composition can lead to different process conditions necessary to obtain optimal results for the reaction and filtration. Therefore, the main aims of this study were to investigate the large number of different qualities of phosphate ore and to identify key process parameters that have a significant impact on phosphoric acid production on an industrial scale (both reactors and UCEGO filters). In addition, to establish connections between these parameters, as well as investigate their relationship with different qualities of phosphate ore, an algorithm was developed to help the broader scientific and engineering community predict the final outcome and quality of the produced acid for any type and quality of phosphate ore, as well as minimize losses of gypsum. This will enable the best process parameters to be found in order to increase the lifespan of phosphate ore and, consequently, lower the energy consumption of the process.

2. Materials and Methods

2.1. Process Simulation of Phosphoric Acid Production

To obtain the model and simulation, the software tools Matlab (version 2021b), SciLab (version 6.1.1), and Aspen Plus (version V12) were utilized. Each model was developed as a rigorous model, where all operating conditions and balances were taken into account to match the industrial conditions. The capacity of the simulation plant was 13,000 P_2O_5 per month or 156,000 tons of P_2O_5 per year.

To ensure the feasibility of this technology and obtain all balances, a complete simulation was performed. For this work, only the reaction and filtration sections were considered. In the production of phosphoric acid, it should be recognized that the process can be divided into two distinct parts. The first part involves the production of diluted phosphoric acid, which plays a pivotal role in determining the quality of the resulting acid and the losses encountered in the gypsum. The second part comprises the vacuum evaporation process, which aims to concentrate the acid by removing water according to market requirements and desired quality for mineral waste production. Significant consequences arise when the quality of the diluted acid falls below satisfactory limits during the initial stage of acid production. Such a scenario necessitates greater energy consumption during vacuum evaporation and may result in higher gypsum traces within the acid. These gyp-

sum traces can subsequently contribute to the formation of deposits in heat exchangers, ultimately causing a reduction in the capacity of the concentration line. To address these critical factors, this research deliberately focuses on tracking the first part of production, encompassing the reaction and filtration sections. This choice allowed monitoring of the quality of the acid and its losses in gypsum, as these aspects significantly impact the overall process efficiency. Although there are expected differences between simulations and real production, this type of process simulator can be used to obtain reliable results for process operation, thanks to the available methods for modeling, the large component database, and the available thermodynamic packages. Initially, the components that constitute the phosphate composition were separated from the Aspen Plus database as the first step towards creating this simulation. Then, models for the reactor, filter, and separator were developed by combining SciLab unit operations with Aspen Plus. Finally, the operating conditions were chosen to imitate real-life production. To the best of the researchers' knowledge, existing techniques often overlook the intricate interplay and coordination among the various sections of the UCEGO filter. They tend to focus on individual sections in isolation, without recognizing the potential cross-effects and interferences that can occur. This manuscript seeks to bridge this gap by analyzing and tracking changes in each part of the filter and establishing connections between them. The conventional approach of considering the filter as a single entity is not sufficient to address the challenges posed by inconsistent filtration quality across different sections.

2.1.1. Experimental Determination of Specific Resistance

To calculate and model the filter and obtain a reliable filter-specific resistance for the process simulation, a laboratory experiment was conducted. Through a series of carefully conducted experiments and referring to the literature [15], we established a correlation between the quantity of filtered acid and the time required for its filtration over the woven material. Determining the gradient and intercept of this correlation enabled us to derive the coefficients used in Equations (1) and (2), which facilitated calculation of the permeability and specific resistance, as demonstrated in the literature [15]. The woven filter used in the experiment was produced by Arena, Valjevo, Serbia.

To obtain a pulp sample, a measuring bottle with a volume of 1 L is used, and the sample is taken directly from the pipeline that supplies the mixture distributor. The bottle's content is poured through a Bihner funnel, where a woven piece is placed, through which filtration takes place (manufacturer: Arena). The time necessary for complete liquid filtration from the pulp was measured using the same vacuum as in the process (Table 1).

Table 1. Experimental values of pulp filterability.

Time, s	14	40.8	52.9	63.2	84	117.4	151.3	196
Volume, L	0.05046	0.1439	0.18505	0.21956	0.28504	0.39575	0.5012	0.63709

The base equations used for calculating permeability and specific resistance are given in Equations (1) and (2), respectively, [15].

$$\text{gradient} = \frac{\alpha_{\text{av}} \cdot c \cdot \mu_l}{{A_f}^2 \cdot \Delta \text{P}_f} \quad (1)$$

$$\text{intercept} = \frac{\mu_l \cdot R}{A_f \cdot \Delta P_f} \quad (2)$$

These equations and experimental values are implemented in the model of the UCEGO filter, Negotin, Serbia. The composition and condition of the filter feed change frequently, and as such, it was necessary to create code that follows and implements these new parameters and their influences on the filtration of phosphoric acid from gypsum cake.

2.1.2. Obtaining Data for Simulation

Only a few articles published in the literature have focused on the composition of phosphate ore, its classification based on the bone phosphate of lime (BPL), and the variation in CaO, P_2O_5, and the mineral composition. Becker [16] addressed this gap and provided an opportunity to utilize the data from his book in simulations to predict and validate the data with real-life production. The primary challenge lies in the fact that varying compositions of a single component in the ore can result in different processes.

In this research, the different quality and composition of phosphate ores as selected from [16] are presented in Table 2.

Table 2. Phosphate compositions used in simulation [16].

Composition/ Phosphate	**Morocco—Khourigba 65–66 BPL**	**Russia Kola 85 BPL**	**Morocco—Khourigba 70–71 BPL**	**Israel—Negev 72 BPL**
H_2O	1.3	1	1.3	0.3
P_2O_5	30.55	39.1	32	33.2
SO_3	1.83	0	1.88	2
F	3.7	2.89	3.9	3.7
SiO_2	2.1	1.2	2.1	1
CO_2	7.1	2	6	4.9
Cl	0.02	0	0.02	0.04
CaO	50.2	50.5	51.2	53
Al_2O_3	0.4	0.85	0.3	0.1
Fe_2O_3	0.2	0.45	0.2	0.05
MgO	0.9	0.12	0.5	0.2
Na_2O	0.9	0.52	0.9	0.7
K_2O	0.07	0.13	0.07	0.01
C(org)	0.21	0	0.22	0
Composition/ Phosphate	**Algeria—Dyobel Onk 65 BPL**	**Brazil 76–78 BPL**	**Algeria—Dyobel Onk 75–77 BPL**	**US—North Carolina 59 BPL**
H_2O	/	/	/	1.3
P_2O_5	29.6	35.8	34.6	28
SO_3	2.4	0	1.6	2.5
F	3.7	1.56	4	3.4
SiO_2	2.4	1.46	2.2	14.4
CO_2	7	4.88	1.2	4.1
Cl	0.02	0.003	/	0.004
CaO	48.5	52.9	54.2	44.1
Al_2O_3	0.4	0.35	0.5	0.4
Fe_2O_3	0.4	0.25	0.4	0.6
MgO	1.4	0.79	0.8	0.5
Na_2O	1.4	0.26	0.6	0.9
K_2O	0.15	0.15	0.01	0.1
C(org)	0.3	0	0	1.6
Composition/ Phosphate	**US—North Carolina 72 BPL**	**Finland 80–81 BPL**		
H_2O	0.2	8		
P_2O_5	32.8	36.8		
SO_3	3	0		
F	3.9	2.6		
SiO_2	1.6	2.7		
CO_2	2.4	4.3		
Cl	0.018	0.006		
CaO	52.5	51.6		
Al_2O_3	0.4	0.3		
Fe_2O_3	0.65	0.6		
MgO	0.63	1.07		
Na_2O	1	0.27		
K_2O	0.12	0.26		
C(org)	0.15	0		

Conversely, numerous articles provide information on and insight into the effects of specific impurities on the reaction and filtration processes [17–21]. Chaabouni's re-

search [21] outlines how the presence of Al_2O_3 and Fe_2O_3 affects filtration, as demonstrated by Equation (3).

$$\frac{Al_2O_3 + Fe_2O_3}{P_2O_5} = from\ 0.08\ to\ 0.1 \quad (3)$$

Low values of Al_2O_3 aluminum promote the growth of gypsum and, consequently, the formation of uniform crystals, thus improving the filtration rate; however, high ratios of aluminum/fluorine increase the viscosity of the acid and its density, which has a detrimental effect on the filtration [21].

The influence of components SiO_2, Al_2O_3, and F [21] on filterability can be predicted by Equation (4).

$$RCF = \frac{\frac{\%F}{19}}{\frac{\%Al_2O_3}{17} + \frac{\%SiO_2}{15}} \quad (4)$$

The filterability of phosphoric muds increases with a decrease in the ratio of fluorine complexation (RCF) within the range of $0.42 \leq RCF \leq 1.378$. This was noted for both raw phosphate 1 (RCF = 0.571) and raw phosphate 2 (RCF = 0.868), where the mass content of acid as P_2O_5 increases and corrosion decreases. However, if the ratio falls below 0.42, the filterability decreases due to the presence of undissolved silica salts and poor crystallization [21].

2.1.3. Description of the Chosen Filter and Separator Model

The UCEGO model is the most commonly used filter in phosphoric acid plants. Its characteristics are listed in Table 3 [22]. Depending on the plant's capacity, filters of various sizes are produced. For this research, type UCEGO No. 9 was selected to model the essential data required to optimize the process (Table 3). Additionally, values such as filter area, number of segments, and diffusivity remain constant. Conversely, variables such as pressure, filter speed, number of segments allocated to each section (controlled by barriers and gondolas), process water flow, process water temperature, and the material flow of strong acid to storage tank vary.

Table 3. UCEGO filter characteristics.

Filter Characteristic							
A/m^2	φT	φf	φf_2	φ_{w1}	φ_{d1}	φ_{w2}	φ_{d2}
109	36	1	8	10	2	9	2
Working Conditions							
		ΔPf/kPa	$xav/\mu m$	$D/m^2\ s^{-1}$	ω/rpm		
		50	20	1×10^{-9}	0.6		

Only one separator, labeled as position 13.01.02 (Figure 1), provides separation of the filtrate and suctioned air through a filter cake for each filtration sector. It consists of two borders, with the first border shorter than the second one, since the liquid level in that section is controlled by the pump speed. When the pump speed is reduced, the level rises and overflows in the second sector (recycled acid), which controls the density and fraction of the H_3PO_4 that returns to the reactor. Thus, the model (model pertains to the B23) was designed to simulate this process and has the ability to change and control the flow of strong acid and transfer excess to the return acid sector. This parameter is critical in phosphoric acid production, since the quality and quantity of recycled acid control the state in the reactor. If there is an insufficient amount of return acid, it can lead to reaction blockage and a rapid rise in density, which can make filtration impossible. Typically, it takes several hours up to a shift to regulate the process when this occurs.

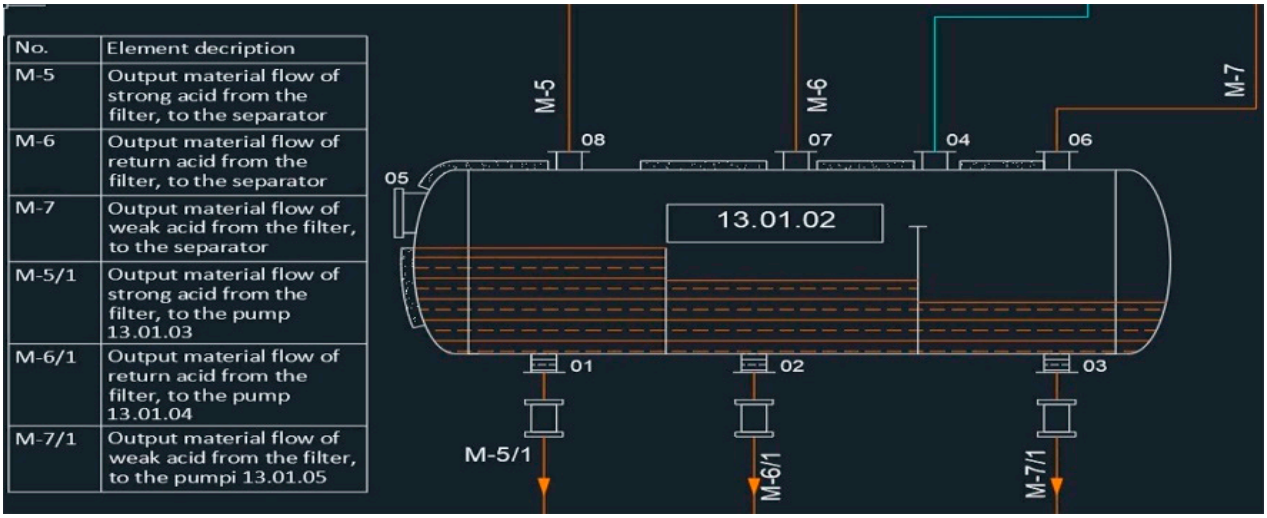

Figure 1. Separator.

2.1.4. Artificial Neural Network

In this study, Artificial neural network (ANN) models were developed to establish a correlation between input parameters and their impact on the production process. The use of an ANN model provides distinct advantages over traditional statistical and regression models. Its advanced capabilities lie in its adaptivity and ability to capture nonlinearity. Given the complexity of parameter changes in the production of phosphoric acid, tracking these changes during regular production becomes challenging. It is noteworthy that altering a single parameter may affect some but not all outlet parameters, while changing multiple input parameters simultaneously may influence other output parameters without affecting the previously modified parameter. To establish a model capable of learning and predicting these intricate relationships, it was deemed necessary to employ an ANN model. By leveraging the adaptive and nonlinear properties, we could effectively discover the connections between these changes. The percentage of samples used for training, validation, and testing was 70%, 15%, 15% respectively, the type of fitting neural network was fitnet, and the type of training algorithm was Levenberg–Marquardt.

The first model was designed to study the filtration process, which included all filtration sections, i.e., strong acid, recycled acid, weak acid, and gypsum disposal sections. This model aimed to identify the combined influence of various parameters on the outlet. The second model focused on monitoring the changes in reactor parameters and their impact on the outlet value. These models were developed separately to address the specific requirements and characteristics of each section. To achieve the best results, the number of neurons in the ANN model was varied from 2 to 30. The ANN model consists of input layers, hidden layers, and output layers.

By employing advanced artificial neural network techniques and employing a multi-objective optimization genetic algorithm, this manuscript aims to optimize the filtration performance across all sections simultaneously, thereby minimizing loss and improving the overall production efficiency. The novelty of this approach lies in its comprehensive nature and the integration of advanced artificial intelligence techniques to address the challenges associated with filtration in phosphoric acid production. To the best of authors' knowledge, no previous studies have specifically focused on developing a model for the UCEGO filter that accounts for the individual sections and their coordination.

2.1.5. Multi-Objective Optimization

The procedure and steps involved in performing multi-objective optimization is presented in Figure 2. The procedure begins with modeling and simulation of phosphoric acid production, where the static change of parameters was achieved (step one). Step two

involves choosing the range of input variables that are going to be used in Aspen Plus by performing sensitivity analysis in order to determine outputs. Using the parameters from the sensitivity analysis, we sought to find correlation between them by implementing Matlab. After creating the ANN model, it was possible to perform code generation in the MATLAB Matrix-Only function, which was later used in the genetic algorithm.

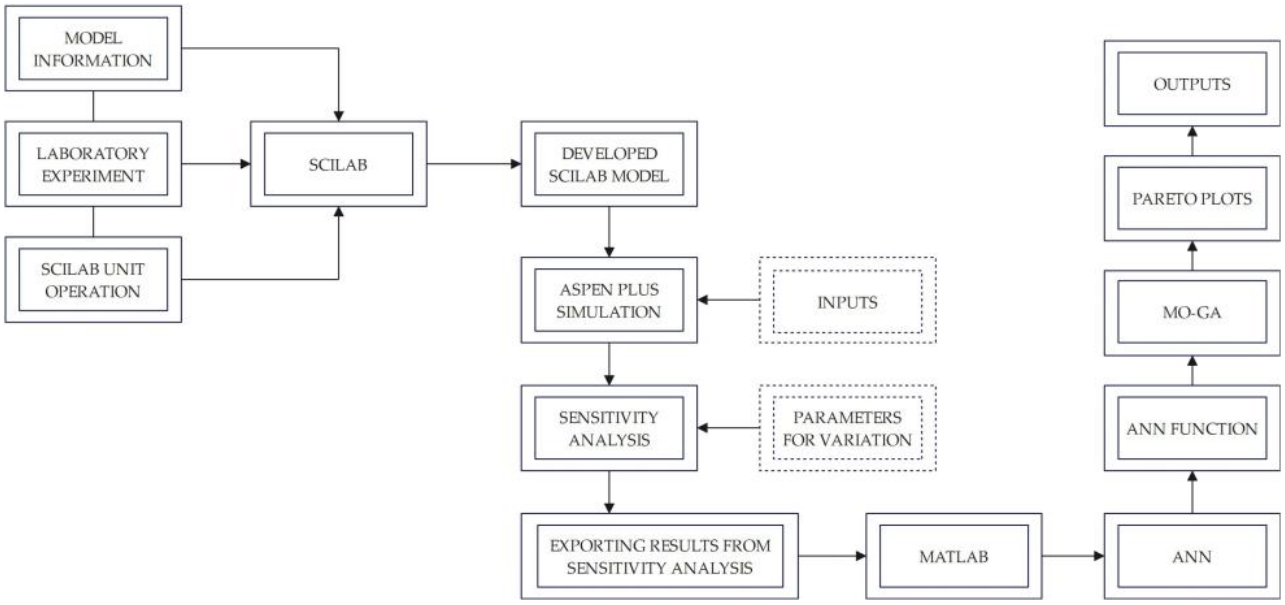

Figure 2. Procedure and steps involved in multi-objective optimization.

The obtained mathematical function is then used in the final step, the multi-objective analysis, employing the selected GA (genetic algorithm) module gamultiobj. The gamultiobj function in MATLAB utilizes a variation of the traditional GA known as the non-dominated sorting genetic algorithm II (NSGA-II). NSGA-II is an elitist algorithm that uses a combination of genetic operators such as selection, crossover, and mutation to evolve a population of candidate solutions. The result is a set of Pareto plots that displays the optimal parameters for phosphoric acid production. The path from modeling to simulation, sensitivity analysis, and ANN, up to MO, is used to solve the next tasks:

1. Limiting loses of phosphoric acid in gypsum;
2. Increasing filtration rate;
3. Achieving high quantity of strong phosphoric acid;
4. Increasing fraction of H_3PO_4 in strong acid.

Procedure

Several objectives were targeted in this multi-objective analysis. First, the reaction and filtration sections were observed independently. As the UCEGO filter consists of several zones, each zone was included, along with its effect on outlets, in the MO analysis.

As mentioned earlier, it is essential to consider the filtration and reaction section as a whole because an alteration in one affects the other. Hence, it was logical to proceed to the second step, which involves tracking the variations of reactor parameters and their impact on filtration.

The final steps involved monitoring the impact of parameter variations in both the reactor and the filter on the quality of the product and the filtration process. Thus, new MO analysis was conducted by taking into consideration the effect of all input changes on output values. This path is presented in Figure 3.

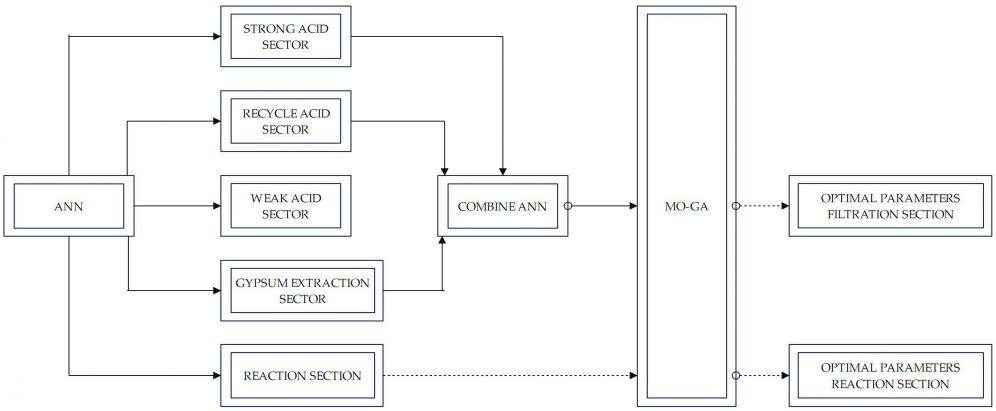

Figure 3. Combined ANN for filtration section.

3. Results and Discussion

3.1. Model Validation

A static simulation of phosphoric acid production, which includes only the reaction and filtration sections, was performed using Aspen Plus. The flow-sheet diagram obtained from Aspen Plus is shown in Figure 4, and a list of the most important block explanations is presented in Table 4.

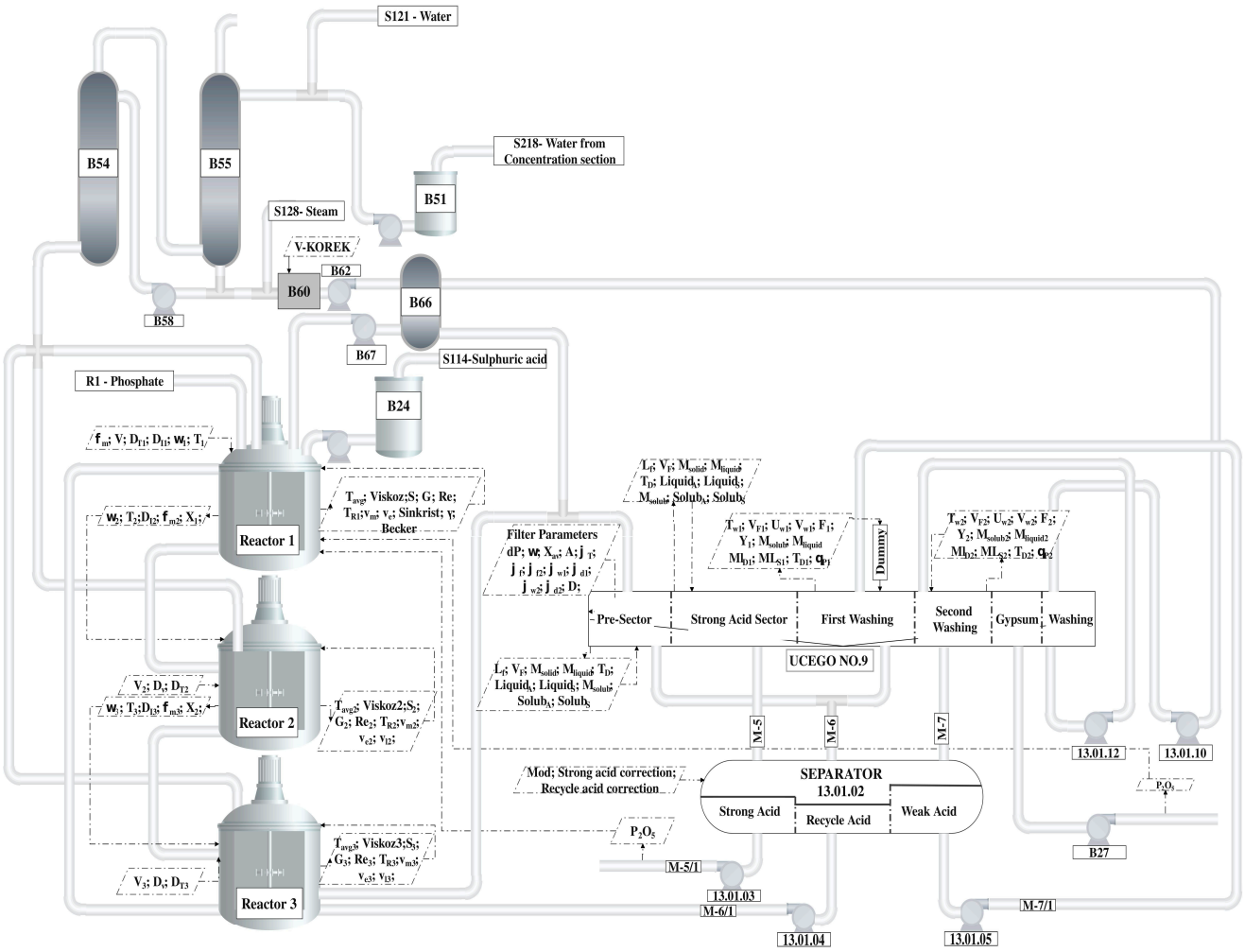

Figure 4. Flow sheet simulation of phosphoric acid production.

Table 4. Model used in Aspen Plus.

Models/Stream	Simulation ID	Model Usage
Reactor 1	Reactor 1	SciLab model of reactor
Reactor 2	Reactor 2	SciLab model of reactor
Reactor 3	Reactor 3	SciLab model of reactor
UCEGO filter	UCEGO	UCEGO filter: for separation of phosphoric acid from gypsum
Pump	13-01-03	Strong acid pump: pump for sending collected strong acid in separator to warehouse
Pump	13-01-04	Return/recycled acid pump: pump for sending collected recycled acid from separator back to reactor
Pump	13-01-05	Weak acid pump: pump for sending collected weak acid from separator to recycled acid sector through filter for washing gypsum cake
Absorber 1	B54	For removing fluoride from gas phase produced in reactor
Absorber 2	B55	For removing fluoride from gas phase produced in reactor
Pump	B58	Pump for sending separated liquid phase from Absorber B54, which is used as washing media
Vacuum cooler	B66	Vacuum cooling is used to cool down part of produced mixture from the reactor, in order to control the temperature in the reactor
Pump	B62	Pump sends water for washing weak acid section through filter
SciLab model	B60	Model control quantity of water sent to the pump B62 and, afterward, to the filter section
H_2SO_4 tank	B24	Storage acid tank
H_2SO_4 pump	B29, B31	Pumps for sending H_2SO_4 to reactor. Depending on necessary capacity, they can work parallel or separately
Separator	B23	SciLab model of separator, which is used to store and separate different types of H_3PO_4 acid removed from UCEGO filter
Pump	B27	Pump sends weak acid as washing medium for recycled acid section through filter
Recycled acid correction	S242	This stream is used in combination with the model of separator B23, as replacement for the frequency regulator of pump 13-01-04, to control the quantity of recycled acid that will be sent back to reactor
Strong acid correction	KOREK	This stream is used in combination with the model of separator B23, as replacement of the frequency regulator of pump 13-01-03, to control the quantity of strong acid that is sent to the storage tank. Excess of acid will overflow to the recycled acid sector in the separator

The phosphoric acid production section can be divided in two parts, the reaction and filtration sections. To perform sensitivity analysis, a separate stream from the SciLab model that represents the final solution or calculated value was created and combined with the Aspen model to maintain material balance. This was necessary, since Aspen cannot recognize the SciLab model and use it directly. For instance, the outlet stream from the UCEGO model, washing section 2 (V_{F2}, U_{W2}, V_{W2}, Y_2, F_2, ML_{S2}, ML_{D2}, T_{W2}, θ_{P2}), represents the calculated parameters, and a "dummy" inlet stream was added to the model to ensure mass balance.

An algorithmic scheme that provides a comprehensive visualization of the model's architecture is included as Supplementary Materials to enhance readers' understanding of the design. This illustrates the different components and their connections, providing a clearer representation of the model's structure.

3.2. Confirmation and Validation of Simulation

The model developed for this simulation was compared to the data from the literature [16] to determine the accuracy. The phosphoric acid production process was simulated under the same conditions used in practice, including ore capacity, H_2SO_4 flow, return acid flow, temperature, return slurry flow, filter speed, water flow for washing the filter cake, vacuum on the filter, temperature of the process water, and other factors.

Table 5 presents a comparison between the simulation results and the literature data. The table indicates an acceptable agreement between the simulation and conditions in real production. Sensitivity analysis was used to identify the optimal solution and the necessary parameters to achieve the results that match those in the literature.

Table 5. Comparison between developed model and the literature.

Morocco—Khouribga 65–66 BPL			**Russia Kolav 85 BPL**			**Morocco-Khouribga 70–71 BPL**		
Component	Model	Literature	Component	Model	Literature	Component	Model	Literature
P_2O_5	29.964	/	P_2O_5	30.1	28	P_2O_5	29.984	30.2
Izrael—Negev 72 BPL			**Algeria—Dyobel Onk 65 BPL**			**Brazil 76–79**		
Component	Model	Literature	Component	Model	Literature	Component	Model	Literature
P_2O_5	29.157	29	P_2O_5	29.915	29.1	P_2O_5	28.456	28
Algeria—Djebel Onk 75–77 BPL			**US—North Carolina 59 BPL**			**US—North Carolina 72 BPL**		
Component	Model	Literature	Component	Model	Literature	Component	Model	Literature
P_2O_5	27.659	27	P_2O_5	26.954	/	P_2O_5	28.637	27.6
Finland 80–81 BPL								
Component	Model	Literature						
P_2O_5	27.659	27						

3.3. Selection of Input Variables for ANN Model

The production of phosphoric acid is a challenging process as it is influenced by numerous parameters, such as the capacity of phosphate, temperature, filter speed, the vacuum on the filter, recycled acid flow, H_2SO_4 flow, strong acid flow, return slurry flow, water for the filtration flow, particle size, steam for heating the water, and water temperature. These parameters were selected as input variables for the sensitivity analysis carried out in Aspen Plus, which generated the results. The value of input variables are given in Tables 6 and 7.

Table 6. Input values for ANN model for phosphoric acid production–filtration section.

Inputs	Value	Extent/Increment
Phosphate ore capacity (ton/h)	70–90	5
Temperature (°C)	65–80	5
Filter speed (rpm)	0.45–0.6	0.03
Vacuum on filter (mbar)	450–600	30
Strong acid flow (ton/h)	60–110	*
Particle size (μm)	4–7	1
Steam flow (ton/h)	3–5	0.5

* Values chosen depending on phosphate ore capacity and the BPL of ore.

Table 7. Input value for ANN model for phosphoric acid production–reaction section.

Inputs	Value	Extent/Increment
Phosphate ore capacity (ton/h)	70–90	5
Temperature (°C)	65–80	5
Recycled acid flow (ton/h)	240–290	10
H_2SO_4 flow (ton/h)	55–78	*
Strong acid flow (ton/h)	60–100	*
Return slurry flow (ton/h)	8–9.5	0.3
Filtration water flow (ton/h)	70–120	*

* Values chosen depending on phosphate ore capacity and the BPL of ore.

All inputs were changed as specified in Tables 6 and 7. Depending on the phosphate ore capacity and type of phosphate, H_2SO_4 flow increased by 1–3%, according to Becker [16]. For values such as filtration water flow and strong acid flow, parameters were chosen depending on phosphate ore capacity and the BPL of ore.

3.3.1. Effect of Pressure on Filtration

The pressure effect on filtration is illustrated in Figure 5. Figure 5a shows that as the vacuum pressure increases, the fractional separation of soluble components decreases. This occurs due to a decrease in specific resistance and permeability of the solid phase, leading to insufficient separation. Following the strong acid sector, the superficial velocity (u) in the return and weak acid sectors decreases, since it is directly proportional to pressure, causing a further decrease in liquid pore velocity (v). The decrease in these parameters results in a reduction of Reynolds and Smith numbers, Dl/D, Dn, and W, which in turn leads to a decrease in fractional efficiency (F). In this work, *F1* represents the first washing section, and *F2* the second washing section. The permeability of soluble components needs to be minimized. As shown in Figure 5, increasing the vacuum pressure results in a decrease in the fractional separation of soluble components due to the decrease in specific resistance and permeability of the solid phase. After the strong acid sector, in the return acid and weak acid sector, the superficial velocity is decreased due to its direct proportionality to pressure, leading to further decreases in liquid pore velocity. Applying a higher vacuum pressure will lead to the most soluble components, along with gypsum, ending up in the gypsum warehouse (Figure 5), but this also represents a loss of economy.

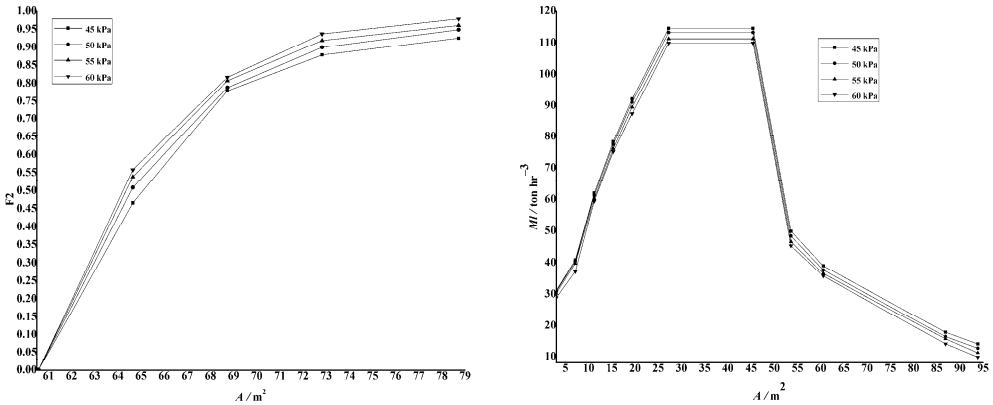

(**a**) (**b**)

Figure 5. Influence of pressure on (**a**) fractional separation of soluble components and (**b**) permeability of liquid components.

3.3.2. Effect of Filter Speed on Filtration

The influence of filter speed on the quantity of separated liquid, cake thickness, and throughput of the liquid and solute phase during the filtration process is shown in Figures 6 and 7. With a decrease in the filter speed, higher separation of liquid Vf from pulp is achieved, reducing liquid and solid throughput, Ml and Ms, respectively.

Decreasing the liquid phase's throughput leads to a higher separation of H_3PO_4 in strong acid (material flow M-5/1, Figure 4). This separation step is crucial for the second wash (material flow M-7/1, Figure 4) since all quantities left unused from the return acid and weak acid sector end up in gypsum (material flow M-10, Figure 4) and represent losses in production. Compensation for the concentration of H_3PO_4 in the return acid (material flow M-6/1, Figure 4) involves reducing the strong acid flow to the storage tank. As a result, some of the strong acid that is not directed to the storage tank overflows into the separator section of the return acid.

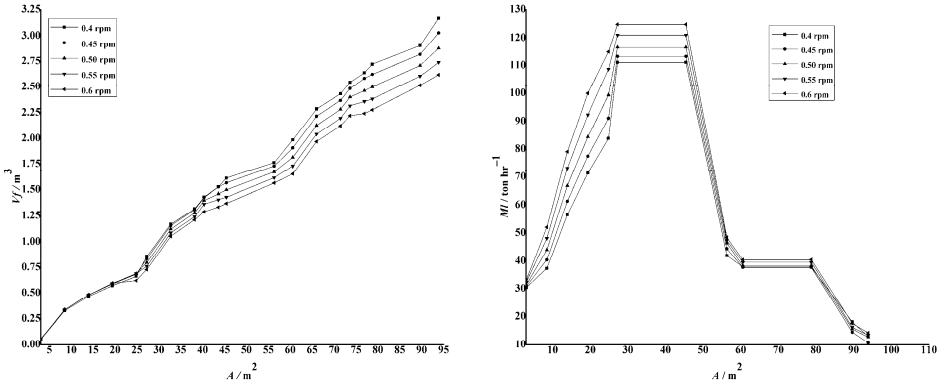

(**a**) (**b**)

Figure 6. Influence of filtration speed on (**a**) amount of separated liquid and (**b**) liquid-phase throughput.

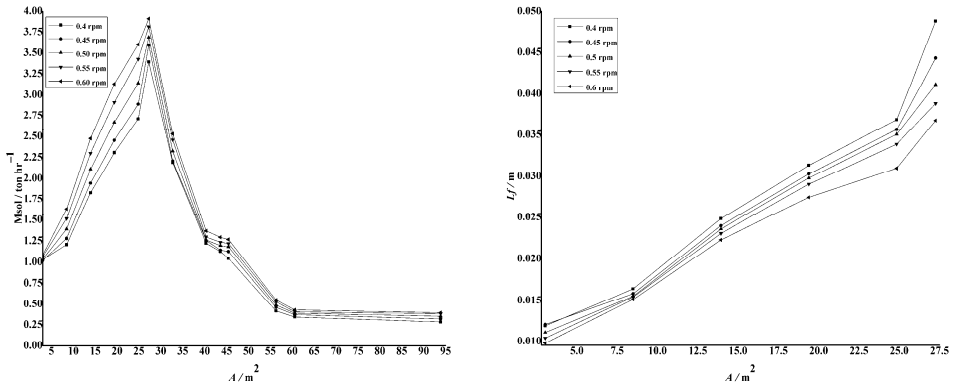

(**a**) (**b**)

Figure 7. Influence of filtration speed on (**a**) amount of separated soluble and (**b**) cake thickness.

3.3.3. Process Water Temperature Effect on Return Acid and Weak Acid Sector

The diagram in Figure 8 illustrates the effect of the process temperature on the fractional separation of soluble components. As the temperature of the process water (material flow M-3, Figure 4) increases, the viscosity and density of the acid decrease. This results in an increase in surface acceleration, which is inversely proportional to viscosity and density. As a result, the superficial velocity increases, leading to an increase in liquid pore velocity. Consequently, the liquid pore velocity is directly proportional to the relationship of Re/Sc, which causes an increase in Dn and results in the change in W and F.

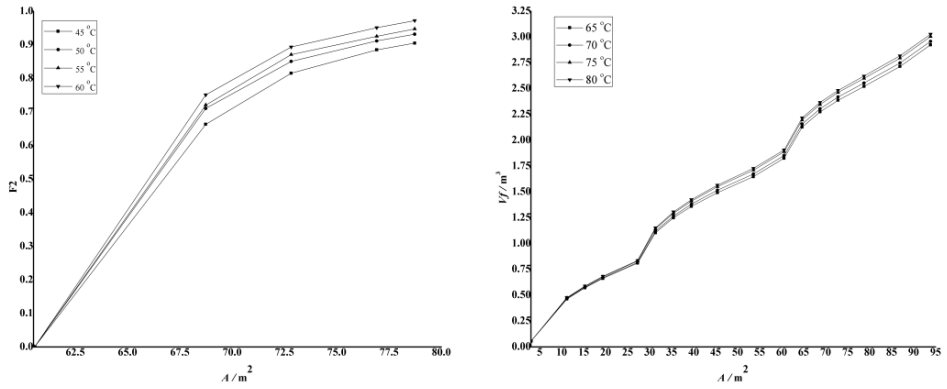

(**a**) (**b**)

Figure 8. Influence of process water temperature on (**a**) fractional separation of soluble components and (**b**) amount of separated liquid from filtration cake.

Higher temperature of the process water (material flow M-3, Figure 4) benefits the filtration process. It increases fraction recovery of soluble components, as the liquid quantity separates from the gypsum cake (Figure 8). As a result, the process loss is minimized by decreasing the throughput of soluble components.

3.3.4. Influence of Filter Feed Temperature

Figure 9 illustrates how the temperature of the feed flow (material flow Slurry, Figure 7) affects the cumulative volume of filtrate. Increasing the temperature of the feed flow, as described in the previous chapter, reduces the viscosity and density of acid, resulting in a higher cumulative volume of filtrate. The temperature was varied at four points: the lowest temperature of 65 °C, which represents the temperature achieved when the process starts after a technical day or equipment washing, and the highest temperature of 80 °C, which is maintained during the production process.

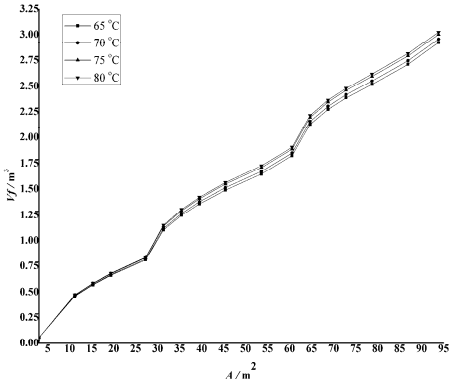

Figure 9. Influence of inlet temperature on amount of separated liquid from filtration cake.

3.4. ANN Development

Complete Filtration and Reaction Section

The first step was to develop an ANN topology for the complete filtration section by changing the filtration section parameters and separately changing the reaction section parameters. After conducting sensitivity analysis in Aspen Tech simulation software, the Matlab toolbox was utilized. The goal of the evaluation was to find the mean square error and correlation coefficient (R) to determine the best performance of the ANN. As R approaches 1, the gap between predicted and actual data decreases, and as R approaches 0, it indicates a mismatch between the two sets of data. Figures 10 and 11 illustrate the ANN topology based on changes in the filtration and reaction section parameters. It was necessary to manipulate the number of hidden neurons to find the best correlation.

For the filtration section, the inlet parameters of the ANN topology include temperature, vacuum, filter speed, particle size, steam flow, strong acid flow, and phosphate ore capacity. These parameters were iterated and used to determine the outlet parameter values, which include cake thickness, strong acid flow, M_{SOLID}, M_{LIQUID}, M_{SOLUB}, H_3PO_4 in strong acid, gypsum in strong acid, % H_3PO_4 in strong acid, and SO_4 in strong acid.

The recycled acid sector is located after the strong acid section and is considered one of the most crucial parts of the process, since its quality can impact the conditions in the reactor and affect the filtration process, resulting in lower quality of strong acid and higher losses of P_2O_5 in gypsum. The outlet monitored parameters include the extracted recycled acid, the concentration of H_3PO_4 in the extracted acid, the recycled acid sent to R1, the concentration of H_3PO_4 in the acid sent to R1, *F1*, *Y1*, *MLD1*, and *MLS1*.

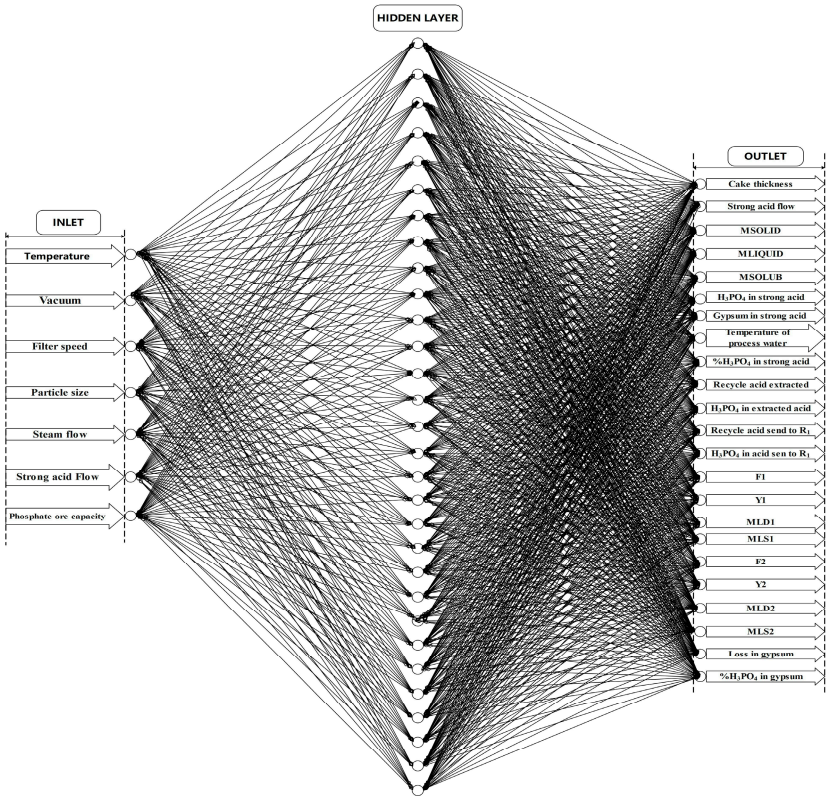

Figure 10. ANN model for all sectors—filtration section parameters.

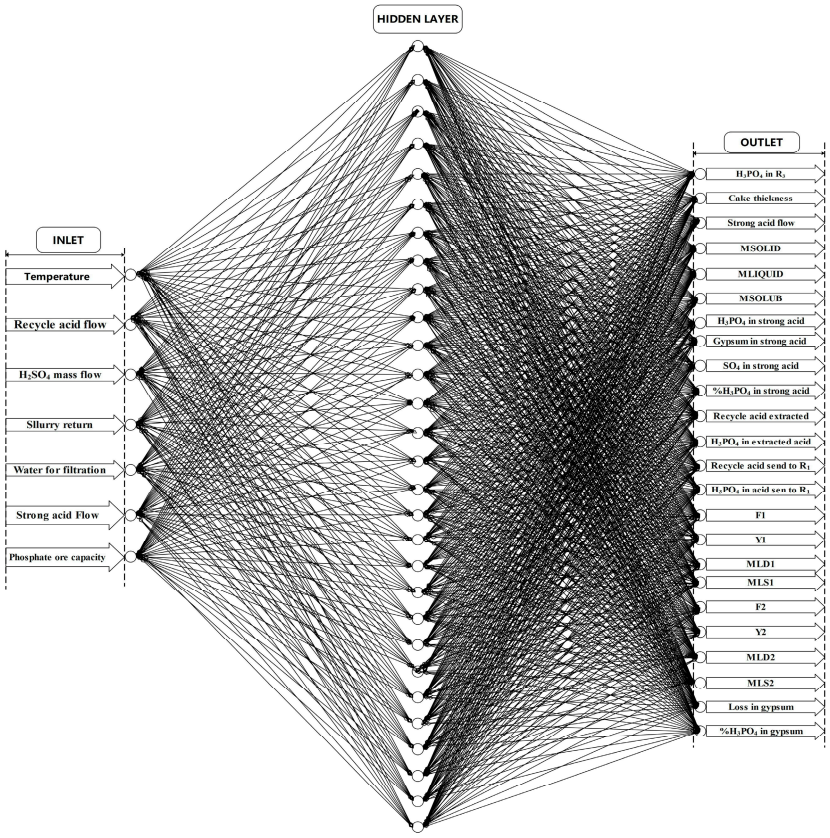

Figure 11. ANN for all sectors—reaction section parameters.

The section that follows the recycled acid sector is the weak acid sector, and its significance in the filtration process cannot be overlooked. If the process quality in this section is satisfactory, it minimizes the loss of phosphoric acid in gypsum and improves the quality of the recycled acid and, consequently, the reactor's condition. The outlet parameters that must be monitored include *F2*, *Y2*, *MLD2*, *MLS2*, and the temperature of the process water.

The last section under the vacuum is the gypsum section; the quality of the gypsum is an indicator of how the reaction and filtration processes have performed. If a large amount of phosphoric acid remains in the gypsum, it indicates that something went wrong during the reaction and filtration processes, and prompt action is required to reduce losses. The monitored outlet values are the H_3PO_4 loss in gypsum (ton/h) and the fraction of H_3PO_4 removed with gypsum from the filter.

The degree of correlation achieved for the filtration and reaction sections is 0.94655 and 0.97667, respectively, using 29 hidden neurons, as shown in Figure 12.

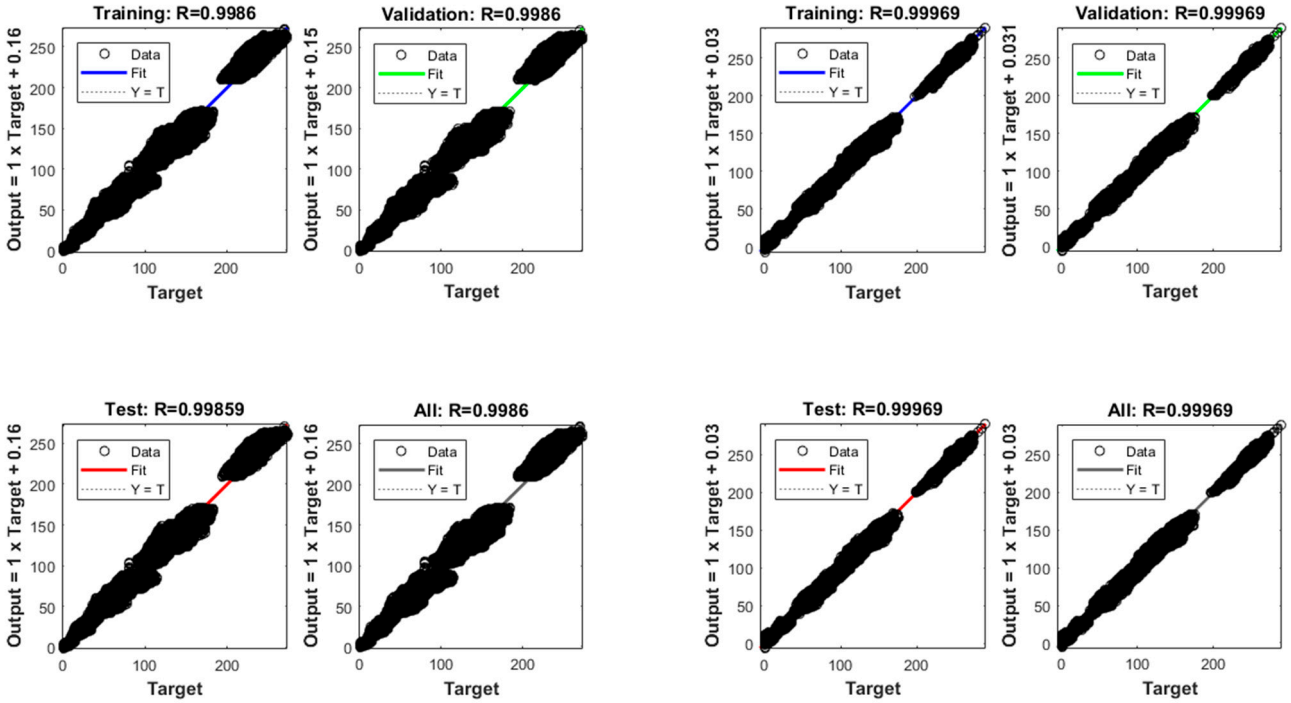

Figure 12. ANN results for all sectors: (**a**) filtration section parameters and (**b**) reaction section parameters.

Disconnection on the parameter line is caused by the parameters between (210–240 ton/h) not being taken in consideration. These parameters represents recycled acid flow. As we used phosphate ore capacity between 70 ton/h and 90 ton/h, the recycled acid flow sent to the reactor must consider roughly three times this capacity, or at least 240 ton/h. The maximum capacity of recycled acid flow sent to the reactor is constrained by the pump capacity, which is 300 ton/h, and by the fact that the more recycled acid that is sent to the reactor, the lower the average resident time in reactor and, consequently, the lower the conversion degree. In a phosphoric acid plant, the ideal resident time is 3 h to 9 h, depending on the volume of the reactor and the capacity of the plant. As it is possible to produce more recycled acid by lowering the output of strong acid to the warehouse and increasing the quantity of water for washing the filtration cake, with pump construction constraints, this would lead to increased levels of fluid in the separator, causing the three sections to be mixed. This mixing will decrease the concentration of acid sent back to the

reactor, lowering the density of pulp and leading to a low conversion degree of P_2O_5 from phosphate ore. After acid is mixed in the separator, filtration on first and second washing sections is disturbed, leading to poor extraction of H_3PO_4 from pulp and high losses of acid in the gypsum. Figure 12 shows correlation between the results of the sensitivity analysis and the parameters predicted with ANN.

3.5. MO (Multi-Objective Analysis)

3.5.1. MO (Multi-Objective Analysis Using GA) Strong Acid Sector

In Figure 13a, the correlation between the extracted H_3PO_4 and gypsum in the strong acid material flow (F-5-1, Figure 4) is shown. The main objective of the process is to achieve the highest quantity and fraction of extracted H_3PO_4 in the material flow (F-5-1, Figure 4). To achieve this goal, it is necessary to increase M_{SOLID} and decrease M_{LIQUID}. However, finding the best compromise of many parameters, such as filtration speed, cake thickness, density of infeed material flow, quantity of infeed, concentration of solids in infeed, viscosity, and vacuum pressure on the filter, is necessary. All these parameters are interdependent and will change during the filtration process, highlighting the complexity of achieving the desired results during the production process.

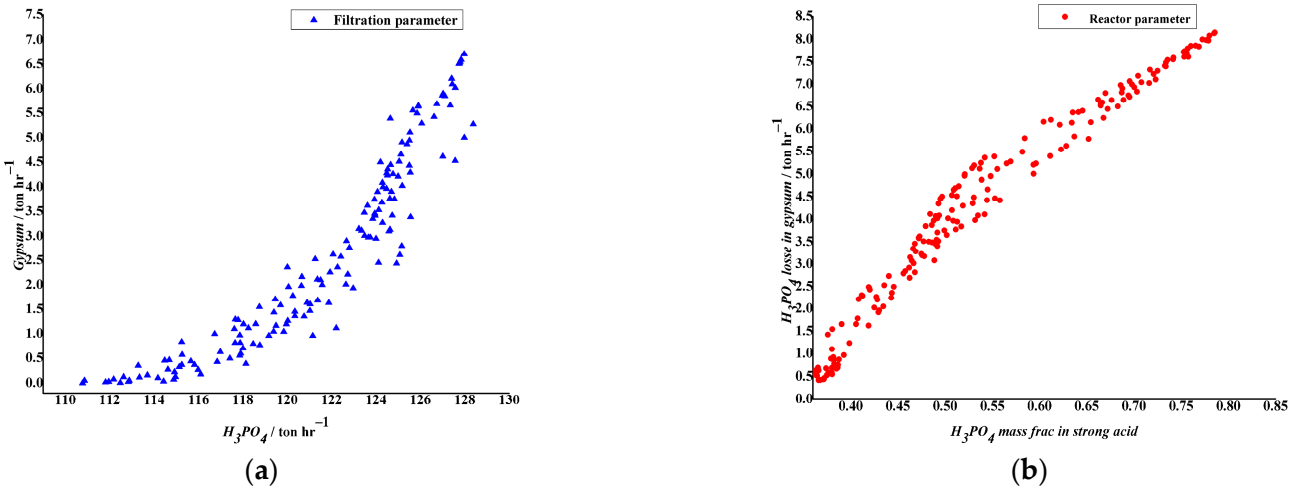

Figure 13. (**a**) MO correlation between extracted H_3PO_4 and gypsum in strong acid material flow achieved by changing filtration parameters; (**b**) MO correlation between fraction of H_3PO_4 in strong acid and losses of acid in gypsum.

As shown in Figure 13, increasing the fraction of H_3PO_4 in the strong acid leads to an increase in the losses of acid in gypsum. To achieve a high mass fraction of phosphoric acid in the strong acid, it is necessary to increase the density and mass fraction of H_3PO_4 that is returned to the reactor as recycled acid. This requires reducing the quantity of strong acid that is sent back to the warehouse, so that all excess acid that is not sent can move to the recycled acid sector, increasing its density and H_3PO_4 fraction. However, when the recycled acid with these characteristics is sent back to the reactor, it can cause blockage of the reaction, requiring more H_3PO_4 and leading to the creation of smaller gypsum crystals, which impairs filtration. This also increases the quantity of H_3PO_4 in the slurry from the reactor to the filter. Therefore, a faster filter rotation speed is required, which reduces the time for filtration in each section, ultimately leading to an increase in the quantity of H_3PO_4 in gypsum. However, this may cause the filter to reach its capacity and fail to extract the required quantity of H_3PO_4 from the slurry before it reaches the final section (gypsum section).

In Table 8, case scenarios are presented regarding the relation between H_3PO_4 extracted from the filter and losses of phosphoric acid in gypsum, achieved by using the optimtool in Matlab and the gamultiobj (multiobjective optimization using genetic algorithm) solver.

It is clear how important the difference between the extracted acid and the acid sent to warehouse is in the quantity of H_3PO_4 lost in gypsum. When there is a significant difference, all acid not used will be held in the separator and poured from the strong acid sector to the recycled acid sector. If the mass fraction of P_2O_5 (main component of H_3PO_4) increases to above 19%, it will lead to larger losses of gypsum, since not all P_2O_5 will manage to react, nor will it be possible to extract it from the filter (considering the construction limitations of the filter). In order to lower the speed filtration and to allow time for each section to perform at an optimal level, the thickness of the gypsum cake must be 4–5 cm. Lowering the rotation speed of UCEGO can lead to an increase in cake thickness, resulting in even worse filtration conditions; this is mostly influenced by the capacity of the phosphate ore. Lowering the capacity of the plant can lead to better filtration; however, economic considerations often lead to a demand for increased production.

Table 8. MO GA optimized parameters between produced strong acid and losses of phosphoric acid in gypsum.

	Filtration Parameter	
	Min	**Max**
Phosphate Ore Capacity (ton/h)	74.13048	74.7
Temperature (°C)	78.312	78.07
Vacuum (kPa)	51	51.21
Filter speed (rpm)	0.54	0.41
Particle size (μm)	5.69×10^{-5}	5.4×10^{-5}
Steam flow (ton/h)	4.687	4.682
Strong acid flow (ton/h)	90.4	91.08
H_3PO_4 (ton/h)	124.19863	110.862
H_3PO_4 losses in gypsum (ton/h)	4.5004	0.055

In Table 9, some case scenarios for the reaction section are presented regarding mass fraction of H_3PO_4 in strong acid and losses of phosphoric acid in gypsum, as determined using the optimtool in Matlab and the gamultiobj (multiobjective optimization using genetic algorithm) solver. Besides the maintenance of temperature, slight changes in the flow of recycled acid, H_2SO_4, and water for filtration, as well as the difference between extracted and used strong acid, can significantly impact the quality of the produced acid and its losses.

First, the flow of recycled acid in the reactor has a significant impact on the reaction and, subsequently, the filtration condition. If the recycled acid has a sufficient concentration of P_2O_5 and flow is between 2.7–3 times the capacity of ore, reaction and filtration conditions will be of such that the filtration is optimized. If there is insufficient recycled acid to be sent to the reactor, the density of the pulp will dramatically increase, leading to worsening of filtration conditions and consequently leading to an even smaller extraction of acid from the recycled acid section, finally causing reaction blockage.

Second, the flow of H_2SO_4 can either lead to satisfactory reaction utilization or to its blocking. The excess SO_4^{2+} in strong acid must be 2.2–2.6%. If there is too little acid added to the reactor, then it will lead to poor reaction efficiency and excess of non-reacted P_2O_5 and CaO. On the other hand, an excess of H_2SO_4 added to the reactor will cause gypsum to surround P_2O_5 particles, preventing conversion to H_3PO_4 and leading to losses of this element in the gypsum.

Table 9. MO GA optimized parameters between mass fraction of H_3PO_4 in produced strong acid and losses of phosphoric acid in gypsum.

	Reaction Parameters	
	Min	**Max**
Phosphate Ore Capacity (ton/h)	86.489	88.554
Temperature (°C)	73.9	76.26
Recycled acid flow (ton/h)	227.14	250.565
H_2SO_4 mass flow (ton/h)	69.128	65.5
Strong acid flow (ton/h)	85.3	89.6
Slurry return (ton/h)	8.06	11.99
Water for filtration (ton/h)	76.03	82.65
H_3PO_4 mass fraction in strong acid	0.464	0.385
H_3PO_4 losses in gypsum (ton/h)	3.078	0.672
F1	0.928	0.943
F2	0.932	0.936
SO_4 fraction in strong acid	0.0165	0.026

3.5.2. Multi-Objective Analysis Using GA: Recycled Acid Sector

In Figure 14, a correlation is shown between liquid throughput and fractional solute recovery (*Y1*) and between solute throughput and fractional solute recovery in the recycled acid sector's first washing sector. The main objective of the process is to achieve the lowest liquid and solute throughput and the highest fractional solute recovery, which will result in the highest possible amount of liquid and soluble phase extracted from the filter cake in the first washing sector. This will increase the concentration of the recycled material flow (F-6-1, Figure 4) and, consequently, the concentration of phosphoric acid in the reactor. Depending on the quality of the phosphate, different compositions and quantities of recycled acid need to be sent back to the reactor. The quantity of recycled acid necessary to be returned to reactor can be calculated in accordance with Becker [16]. All equations are presented in the Supplementary Materials.

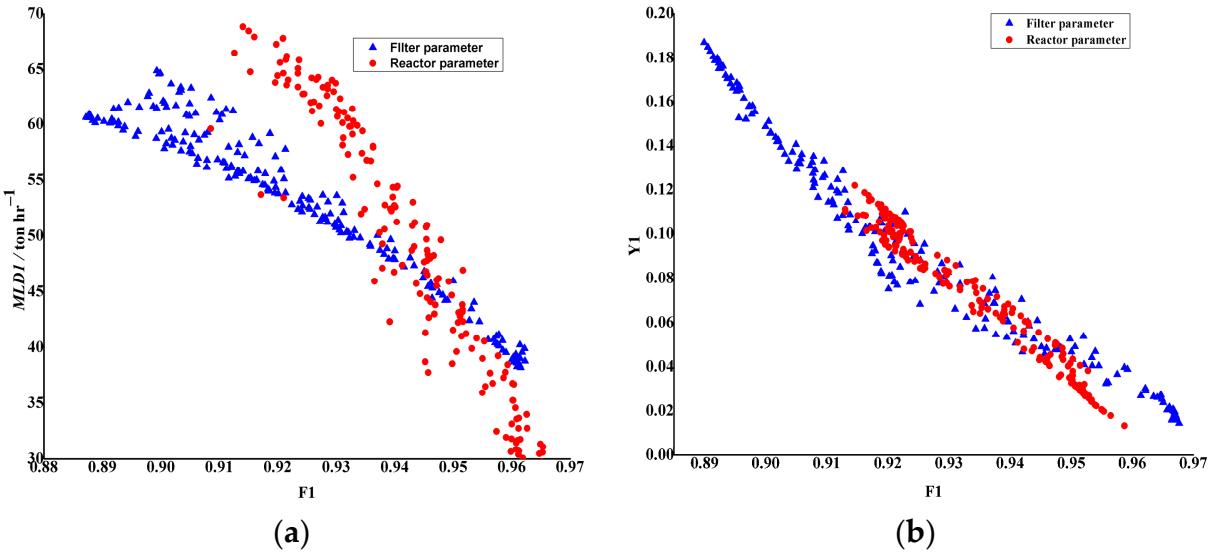

Figure 14. (**a**) MO correlation between throughput of liquid and fractional solute recovery achieved after changing filtration and reaction parameters, (**b**) MO correlation between Y1 and fractional solute recovery achieved after changing filtration and reaction parameters.

In Tables 10 and 11, some case scenarios for the reaction and filtration sections are presented regarding the relation between throughput of liquid and fractional solute, and Y1 and fractional solute recovery, determined using optimtool.

Table 10. MO GA optimized parameters between throughput of liquid and fractional solute for first washing section, including best- and worst-case scenarios for filtration and reaction parameters.

Filter Parameters			Reaction Parameters		
	Min	**Max**		**Min**	**Max**
Phosphate ore capacity (ton/h)	70.00995	89.992949	Phosphate ore capacity (ton/h)	70.0267	89.76
Temperature (°C)	79.048895	70.058808	Temperature (°C)	79.629	75.84
Vacuum (kPa)	54.984397	45.002289	Recycled acid flow (ton/h)	240.896	254.99
Filter speed (rpm)	0.407062	0.402549	H_2SO_4 mass flow (ton/h)	60.1	74.54
Particle size (µm)	5.59×10^{-5}	4.05×10^{-5}	Strong acid flow (ton/h)	70.023	87.5
Steam flow (ton/h)	4.594334	4.0367736	Slurry return (ton/h)	11.98	11.7
Strong acid flow (ton/h)	94.972762	61.679838	Water for filtration (ton/h)	83.39	73
F1	0.9625254	0.8673016	F1	0.968	0.913
MLD1 (ton/h)	36.574536	73.55024	MLD1 (ton/h)	27.016	0.111

Table 11. MO GA optimized parameters between Y1 and fractional solute recovery for first washing section, including best- and worst-case scenarios for filtration and reaction parameters.

Filter Parameters			Reaction Parameters		
	Min	**Max**		**Min**	**Max**
Phosphate ore capacity (ton/h)	70.00856	89.982	Phosphate ore capacity (ton/h)	70	89.76
Temperature (°C)	79.4	71.36	Temperature (°C)	79.004	75.84
Vacuum (kPa)	54.9	45.057	Recycled acid flow (ton/h)	246.93	255
Filter speed (rpm)	0.548	0.402	H2SO4 mass flow (ton/h)	60	74.54
Particle size (µm)	5.6×10^{-5}	4.02×10^{-5}	Strong acid flow (ton/h)	70.2	87.5
Steam flow (ton/h)	4.468	4.521	Slurry return (ton/h)	12	11.7
Strong acid flow (ton/h)	72.9	65.1	Water for filtration (ton/h)	70	73
F1	0.9676	0.889	F1	0.9587	0.913
Y1	0.0146	0.1871	Y1	0.0134	0.112

First, the influence of temperature is absolute; by increasing temperature, we achieve higher yield in the reactor, which consequently leads to better filtration conditions. The temperature should be over 80 °C as this will lead to a loss of one molecule of water in gypsum, which should be avoided. At above 82 °C, gypsum will lose both molecules of water.

Second, vacuum and filter speed are the main parameters on the UCEGO filter. It is mandatory to adjust these such that thickness of gypsum cake is between 4–5 cm. If speed is too low in comparation to phosphate ore capacity, the filter cake can become almost non-filtrable, which leads to high losses.

Third, particles can have different shapes and sizes, depending on the reaction conditions and recycled acid sent back to reactor. Small crystals such as the needle type will lead to blockage of pores on the woven filter, causing bad filtration and increasing losses of acid in gypsum. On the other hand, bigger plate-like crystal will benefit the process of filtration, increasing the mass fraction of H_3PO_4 in strong acid and leading to smaller losses in gypsum.

Forth, steam is used to preheat the water that is used for washing the gypsum cake. This water will first be sent to the second washing section, and after filtration, move to the first washing section; see Figure 8. For the filtration section, a lower bounds search space of [70 65 45 0.45 4 $\times$ 10^{-5} 3 60] was established, while the corresponding upper bounds were [90 80 60 0.6 7 $\times$ 10^{-5} 5 110]. These bounds ensure that the algorithm's search is confined within a reasonable and meaningful range.

Similarly, for the reaction section, the lower bounds search space was set as [70 65 240 55 60 8 70], while the upper bounds were [90 80 270 78 100 9.5 100]. These bounds were carefully chosen to maintain the feasibility and practicality of the algorithm's exploration in the reaction domain.

3.5.3. Multi-Objective Analysis Using GA: Weak Acid Sector

Figure 15a shows the correlation between liquid throughput–fractional solute recovery, and Figure 15b shows the Y2–fractional solute recovery in the weak acid sector and second washing sector. The main goal of process is to achieve the lowest throughput of liquid and highest fractional solute recovery. By achieving this, in the second washing sector, the lowest possible amount of liquid and soluble phase will be left in the filter cake as gypsum waste from the filter. If this is not achieved, a higher quantity of phosphoric acid will remain trapped in the filtration cake before the last section, which removes the gypsum from the filter. This represents losses in the production process; depending on capacity, such losses can be significantly large.

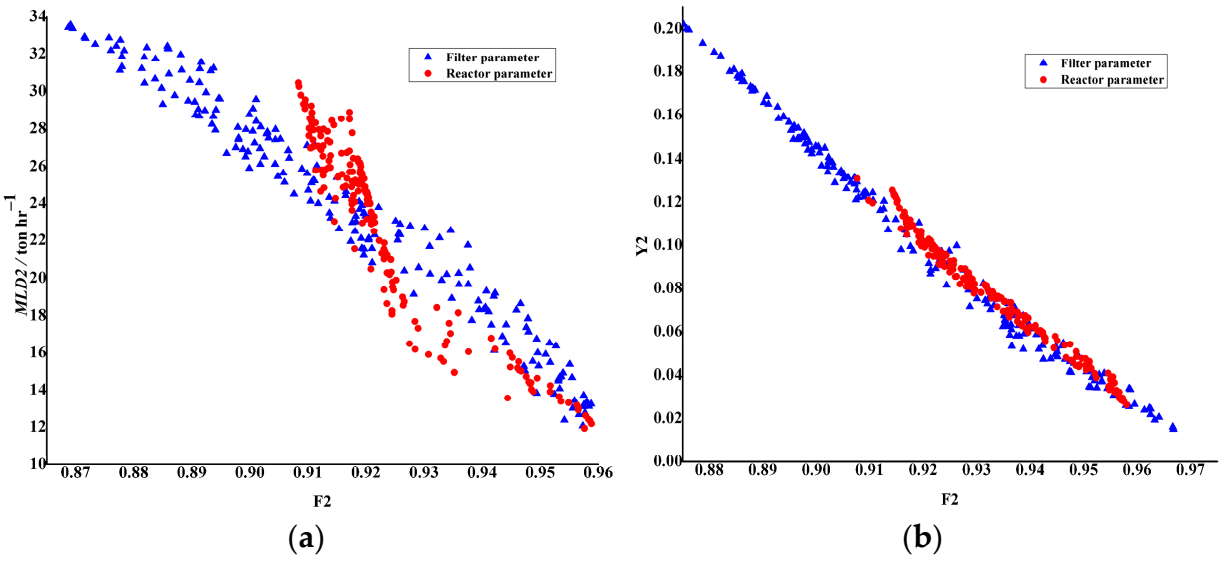

Figure 15. (**a**) MO correlation between throughput of liquid and fractional solute recovery achieved after changing filtration and reaction parameters; (**b**) MO correlation between Y2 and fractional solute recovery achieved after changing filtration and reaction parameters.

In Tables 12 and 13, case scenarios for the reaction and filtration sections are presented regarding the relation between the throughput of liquid and fractional solute, and Y2 and fractional solute recovery, for the second washing section, achieved using the same optimization tools as in previous chapters.

Table 12. MO GA optimized parameters between throughput of liquid and fractional solute for second washing section, including best- and worst-case scenarios for filtration and reaction parameters.

Filter Parameters				Reaction Parameters	
	Min	**Max**		**Min**	**Max**
Phosphate ore capacity (ton/h)	70.06	89.97166	Phosphate ore capacity (ton/h)	83.01	88.6
Temperature (°C)	78.4069	74.60292	Temperature (°C)	79.878	76.9
Vacuum (kPa)	54.922	45.40905	Recycled acid flow (ton/h)	265.2	265.3
Filter speed (rpm)	0.4374	0.416919	H2SO4 mass flow (ton/h)	60.23	73.7
Particle size (μm)	5.85×10^{-5}	4.05×10^{-5}	Strong acid flow (ton/h)	60.23	74
Steam flow (ton/h)	4.933	4.118	Slurry return (ton/h)	11.8	9.05
Strong acid flow (ton/h)	70.2	74.257	Water for filtration (ton/h)	77.36	84.46
F2	0.9587	0.86873	F2	0.9588	0.9083
MLD2 (ton/h)	13.2291	33.43067	MLD2 (ton/h)	12.176	30.436

Table 13. MO GA optimized parameters between Y2 and fractional solute recovery for second washing section, including best- and worst-case scenarios for filtration and reaction parameters.

Filter Parameters				Reaction Parameters	
	Min	**Max**		**Min**	**Max**
Phosphate ore capacity (ton/h)	70.827	88.827	Phosphate ore capacity (ton/h)	83.73	88
Temperature (°C)	77.3488	70.58	Temperature (°C)	77.46	70.44
Vacuum (kPa)	53.9089	45.68	Recycled acid flow (ton/h)	276.1	261.6
Filter speed (rpm)	0.51308	0.4352	H2SO4 mass flow (ton/h)	60.107	74.07
Particle size (μm)	6×10^{-5}	4.06×10^{-5}	Strong acid flow (ton/h)	95.5	73.6
Steam flow (ton/h)	4.794	4.275	Slurry return (ton/h)	11.4	10.5
Strong acid flow (ton/h)	88.4	60.5	Water for filtration (ton/h)	77.27	79.05
F2	0.9667	0.8751	F2	0.958	0.90763
Y2	0.01512	0.202	Y2	0.0264	0.1308

The study demonstrates the feasibility of predicting the influence of process parameters on the quality of produced acid and minimizing losses during production. The viability of the developed model was confirmed through comparison with results reported in the literature.

4. Conclusions

The developed model and simulation have the potential to forecast process parameters and conditions in reactors and UCEGO filters. This presents an opportunity for plants to reduce energy consumption and, more importantly, enhance phosphoric acid extraction while decreasing acid losses in gypsum. By achieving this, the life span of phosphate ore could potentially be extended.

Working conditions of the UCEGO filter and reactor were determined using ANN and multi-objective analysis. Datasets were obtained using compositions of different phosphate ores from literature. The aim was to take in consideration different quality levels of phosphate ore, with different values of BPL, in order to create an achievable method that takes into consideration all relevant advantages and disadvantages.

Using the collected data and process parameters, approximately one million combinations were generated by modifying all feasible parameters during the production of phosphoric acid. This can assist engineers and operators in forecasting the optimal course of action and maintaining it throughout production. Subsequently, ANN models were established, which exhibited a high determination value of over 0.99.

Changing process parameters in this simulation proved to be adequate to decrease losses of H_3PO_4 in gypsum and increase its concentration in the produced acid. Constraints such as temperature in the reactor, mass flow of recycled acid from the filter to the reactor, H_2SO_4 mass flow, water for filtration, strong acid flow, vacuum on the filter, filter speed, and temperature of the filtration water were necessary in order to achieve optimal operation for the filter and reactor, a conversion degree of 96–97%, a fractional solute recovery over 0.96 for both washing sections, and the lowest liquid throughput.

The results achieved can be compared with those in the literature and in phosphoric acid plants, showing that simulation programs such as AspenTech, Matlab, SciLab, and SciLab Unit operation can be used to predict and optimize industrial production.

Supplementary Materials: The following supporting information can be downloaded at: https://www.mdpi.com/article/10.3390/pr11061753/s1.

Author Contributions: Conceptualization, M.P. (Marko Pavlović) and P.K.; methodology, M.P. (Marko Pavlović); software, M.P. (Marko Pavlović); validation, M.P. (Marko Pavlović); formal analysis, M.P. (Marko Pavlović); investigation, M.P. (Marko Pavlović); resources, M.P. (Marko Pavlović); data curation, M.P. (Marko Pavlović), J.L., L.P., M.P. (Milada Pezo), O.B. and P.K.; writing—original draft preparation, M.P. (Marko Pavlović), J.L., L.P., M.P. (Milada Pezo), O.B. and P.K.; writing—review and editing, M.P. (Marko Pavlović), J.L., L.P., M.P. (Milada Pezo), O.B. and P.K.; visualization, M.P. (Marko Pavlović); supervision, J.L. and P.K.; project administration, J.L. and P.K.; funding acquisition, M.P. (Marko Pavlović), J.L., L.P., M.P. (Milada Pezo), O.B. and P.K. All authors have read and agreed to the published version of the manuscript.

Funding: This research received no external funding.

Data Availability Statement: Not applicable.

Acknowledgments: The authors would like to acknowledge the Ministry of Education, Science and Technological Development of the Republic of Serbia for their financial support, Project No. 451-03-47/2023-01/200134.

Conflicts of Interest: The authors declare no conflict of interest.

Nomenclature

A	Filtration area, m^2
A_f	Filtration area of woven filter in Buhner funnel, m^2
ANN	Artificial Neural Network
B	Mass fraction of gypsum per unit mass of slurry in reactor
Becker	Conversion degree in a reactor based on calculation from Becker
c	Solid concentration in feed, kg m^{-3}
D	Molecular diffusivity of solute, m^2 s^{-1}
D_a	Specific gravity of phosphoric acid
D_{I1}	Impeller diameter for Reactor 1, m
D_{I2}	Impeller diameter for Reactor 2, m
D_{I3}	Impeller diameter for Reactor 2, m
D_{T1}	Reactor tank 1 diameter, m
D_{T2}	Reactor tank 2 diameter, m
D_{T3}	Reactor tank 2 diameter, m
dP	Vacuum pressure, kPa
F_1	Fraction of solute removed from a filter cake in washing section 1
F_1	Fraction of solute removed from a filter cake in washing section 2
G	Degree of supersaturation in Reactor 1
G_2	Degree of supersaturation in Reactor 1
G_3	Degree of supersaturation in Reactor 3
G_{di}	Gypsum cake production, gypsum cake/ton rock
I	Impurities apart from the P_2O_5 component in phosphate rock
K_L	Physical mass transfer coefficient of H^+ in solution (m/h)
L_f	The thickness of the filter cake, m

M_{LD1}	Throughput of liquids in filter cake, ton h^{-1}
M_{LD1}	Throughput of liquids in filter cake, ton h^{-1}
M_{LS1}	Throughput of solute in filter cake, ton h^{-1}
M_{Ls2}	Throughput of solute in filter cake, ton h^{-1}
M_{liquid}	Throughput of liquids in filter cake, ton h^{-1}
MO	Multi-objective
M_{solid}	Throughput of solids in filter cake, ton h^{-1}
M_{solub}	Throughput of solute in filter cake, ton h^{-1}
R	Resistance of fluid flow through a filter cloth, m^{-1}
R_{e1}	Reynolds number in Reactor 1
R_{e2}	Reynolds number in Reactor 2
Re_3	Reynolds number in Reactor 3
S	Supersaturation of calcium sulfate in Reactor 1
S_2	Supersaturation of calcium sulfate in Reactor 2
S_3	Supersaturation of calcium sulfate in Reactor 3
T	Temperature in Reactor 1
T_2	Temperature in Reactor 2
T_3	Temperature in Reactor 2
T_{avg}	Average or mean residence time in Reactor 1
T_{avg2}	Average or mean residence time in Reactor 2
T_{avg3}	Average or mean residence time in Reactor 3
T_D	Deliquoring time, s
T_{D1}	Deliquoring time for first section, s
T_{D2}	Deliquoring time for second section, s
T_R	Complete dissolution time of a single particle of radius R, h
T_{R1}	Complete dissolution time of a single particle of radius R in R1, h
T_{R2}	Complete dissolution time of a single particle of radius R in R2, h
T_{R3}	Complete dissolution time of a single particle of radius R in R3, h
T_{w1}	Time of filtration for first washing section, s
T_{w2}	Time of filtration for second washing section, s
U_{w1}	Superficial velocity of a fluid first washing section, m^3 m^2 s^{-1}
U_{w2}	Superficial velocity of a fluid second washing section, m^3 m^2 s^{-1}
V	Volume of reactor 1, m^3
V_2	Volume of reactor 2, m^3
V_3	Volume of reactor 3, m^3
V_f	Filtrate volume—strong acid sector, m^3
V_{f2}	Filtrate volume—second washing sector, m^3
V_{f1}	Filtrate volume—first washing sector, m^3
VISKOZ	Viscosity of reaction solution in Reactor 1, kg m h^{-1}
$Viskoz_2$	Viscosity of reaction solution in Reactor 2, kg m h^{-1}
$Viskoz_3$	Viscosity of reaction solution in Reactor 3, kg m h^{-1}
V_{w1}	Pore velocity of a fluid, first washing section, m s^{-1}
V_{w2}	Pore velocity of a fluid, second washing section, m s^{-1}
V_{si}	Volume of slurry produced in the reactor (slurry/ton rock)
X_1	Conversion degree in a Reactor 1
X_2	Conversion degree in a Reactor 2
X_3	Conversion degree in a Reactor 3
X_{av}	Particle diameter, μm
Greek Letter	
α_{av}	Specific resistance of a filter cake, m kg^{-1}
ΔP_f	Vacuum pressure, kPa
θ_{P1}	Dewatering time—first Deliquoring section, s
θ_{P2}	Dewatering time—second Deliquoring time, s
μ_l	Viscosity of the liquid in a feed, Pa*s
υ_e	Crystal growth rate in Reactor 1, kg h^{-1} m^2
υ_{e2}	Crystal growth rate in Reactor 2, kg h^{-1} m^2
υ_{e3}	Crystal growth rate in Reactor 3, kg h^{-1} m^2
υ_l	Linear crystal growth rate in Reactor 1, m h^{-1}

υ_{l2}	Linear crystal growth rate in Reactor 2, m h^{-1}
υ_{l3}	Linear crystal growth rate in Reactor 3, m h^{-1}
υ_{m1}	Dissolution rate of phosphate rock per unit of particle surface in R1, kg h^{-1} m^2
υ_{m2}	Dissolution rate of phosphate rock per unit of particle surface in R2, kg h^{-1} m^2
υ_{m3}	Dissolution rate of phosphate rock per unit of particle surface in R3, kg h^{-1} m^2
Φ_{m1}	Mineral particle shape factor in Reactor 1
Φ_{m2}	Mineral particle shape factor in Reactor 2
Φ_{m3}	Mineral particle shape factor in Reactor 3
φ_{d1}	Number of filtration segments dedicated to first Deliquoring sector
φ_{d2}	Number of filtration segments dedicated to second Deliquoring sector
φ_{f}	Number of filtration segments dedicated to pre-sector
φ_{f2}	Number of filtration segments dedicated to strong acid sector
φ_{T}	Total number of UCEGO filter segments
φ_{w1}	Number of filtration segments dedicated to first washing sector
φ_{w2}	Number of filtration segments dedicated to second washing sector
ω	Rotation speed of filter, rpm
ω_1	Reactor 1 impeller speed, rpm
ω_2	Reactor 2 impeller speed, rpm
ω_3	Reactor 3 impeller speed, rpm

References

1. Salas, B.V.; Wiener, M.S.; Martinez, J.R.S. *Phosphoric Acid Industry—Problems and Solutions*; InTech: London, UK, 2017.
2. Global Phosphoric Acid Market—Industry Trends and Forecast to 2028. Available online: https://www.databridgemarketresearch.com/reports/global-phosphoric-acid-market (accessed on 8 August 2022).
3. Mathias, P.M.; Mendez, M. Simulation of phosphoric acid production by the dihydrate process. In Proceedings of the 22nd Clearwater Convention on Phosphate Fertilizer & Sulfuric Acid Technology Sheraton Sand Key Resort, Clearwater Beach, FL, USA, 22–23 May 1998.
4. Kannamma, B.; Kannadasan, T.; Prabhakaran, D. Analysis and Simulation of Dihydrate Process for the Production of Phosphoric Acid (Reactor Section). *Am. J. Eng. Res.* **2013**, *2*, 1–8.
5. Messnaoui, B.; Bouhaouss, A.; Derja, A. A Steady State Model for Describing the Phosphate Lattice Loss. *Procedia Eng.* **2012**, *46*, 134–142. [CrossRef]
6. Mathias, P.M.; Chen, C.-C.; Walters, M. Modeling the Complex Chemical Reactions and Mass Transfer in a Phosphoric Acid Reactor. In Proceedings of the Third Joint China/USA Chemical Engineering Conference, Beijing, China, 25–28 September 2000.
7. Papadopoulos, A.I.; Theodosiadis, K.; Seferlis, P. Modeling, Design and Optimisation of Industrial Phosphoric Acid Production Processes. In Proceedings of the 10th Conference on Process Integration, Modelling and Optimisation for Energy Saving and Pollution Reduction, Thessaloniki, Greece, 2007. Available online: https://folk.ntnu.no/skoge/prost/proceedings/icheap8-pres07/pres07webpapers/28%20Papadopoulos.pdf (accessed on 8 August 2022).
8. Bouchkira, I.; Latifi, A.M.; Khamar, L.; Benjelloun, S. Modeling and Multi-Objective Optimization of the Digestion Tank of an Industrial Process for Manufacturing Phosphoric Acid by Wet Process. *Comput. Chem. Eng.* **2022**, *156*, 107536. [CrossRef]
9. Abu-Eishah, S.I.; Abu-Jabal, N.M. Parametric Study on the Production of Phosphoric Acid by the Dihydrate Process. *J. Chem. Eng.* **2001**, *81*, 231–250. [CrossRef]
10. Peng, Y.; Zhu, Z.; Braatz, R.D.; Myerson, A.S. Gypsum Crystallization during Phosphoric Acid Production: Modeling and Experiments Using the Mixed-Solvent-Electrolyte Thermodynamic Model. *Ind. Eng. Chem. Res.* **2015**, *54*, 7914–7924. [CrossRef]
11. Yeo, Y.K.; Cho, Y.S.; Moon, B.K. Simulation of the Dihydrate Process for the Production of Phosphoric Acid. *Proc. Korean Soc. Autom. Control.* **1988**, *1*, 875–878. [CrossRef]
12. Grema, A.S.; Iyodo, H.M.; Grema, A.S.; Imam, Y.Y.; Mohammed, H.I. Modeling and Simulation of Hemihydrate Phosphoric Acid Plant. *Arid Zone J. Eng. Technol. Environ.* **2018**, *14*, 169–171.
13. Papadopoulos, A.I.; Seferlis, P. Generic Modelling, Design and Optimization of Industrial Phosphoric Acid Production Processes. *Chem. Eng.Process. Process Intensif.* **2009**, *48*, 493–506. [CrossRef]
14. Tarleton, E.S.; Wakeman, R.J. *Solid/Liquid Separation*; Elsevier: Amsterdam, The Netherlands, 2007; ISBN 9781856174213.
15. Richard, J.; Wakeman, E.S. *Tarleton Filtration Equipment Selection, Modelling and Process Simulation*, 1st ed.; Elsevier Advanced Technology: Amsterdam, The Netherlands, 1999.
16. Becker, P. *Phosphates and Phosphoric Acid: Raw Materials, Technology, and Economics of the Wet Process. Revised and Expanded*; Marcel Dekker, Inc.: New York, NY, USA, 1989; Volume 6.
17. Kybartiene, N.; Valancius, Z.; Leskeviciene, V.; Urbonas, L. Influence of the composition of phosphate rock on the amount of water-insoluble phosphate impurities in semi-hydrate phosphogypsum. *Ceramics-Silikáty* **2015**, *29*, 29–36.
18. Pyagai, I.; Zubkova, O.; Babykin, R.; Toropchina, M.; Fediuk, R. Influence of Impurities on the Process of Obtaining Calcium Carbonate during the Processing of Phosphogypsum. *Materials* **2022**, *15*, 4335. [CrossRef] [PubMed]

19. Fernandes, N.J.; Galvão, M.A.; Araujo, L.R.; Ataíde, C.H.; Barrozo, M.A.S. Effect of the Impurities on the Phosphoric Acid Process. In *Materials Science Forum*; Trans Tech Publications Ltd.: Stafa-Zurich, Switzerland, 2012; Volume 727, pp. 386–391.
20. Zarenezhad, B. Effect of Impurities in Phosphoric Acid on the Granulometery of the Produced DAP(Di-Ammonium Phosphate) in Petrochemical Plants. *Korean J. Chem. Eng.* **2002**, *19*, 928–931. [CrossRef]
21. Chaabouni, A.; Chtara, C.; Nzihou, C.A.; El Feki, H. Study the Nature and the Effects of the Impurities of Phosphate Rock in the Plants of Production of Phosphoric Acid. *Adv. J. Chem.* **2014**, *7*, 1296–1299. [CrossRef]
22. Little, D.; Berberat, C. *Ucego Filters in Phosphoric Acid Production*; Peninsular Florida Section of the American Institute of Chemical Engineering: Tallahassee, FL, USA, 1981.